Journal of Theoretical and Applied Information Technology
15th May 2021. Vol.99. No 9

ISSN: 1992-8645 www.jatit.org E-ISSN: 1817-3195

INNOVATIONATTITUDE CONTROL OF A HEXACOPTER PLATFORM BASED ON FRACTIONAL CONTROL LAWS AND COMPARISON WITH THE PID AND LQR CONTROL METHODS

[1] SAAD ENNIMA*, [2] SALMANE BOUREKKADI, [3] ASMAE OURDI ,[1] ABDELLAH ELGHARAD

[1] M2SM, Research Center STIS, Dep. of Mechanical Engineering,
ENSAM RABAT (Ex.ENSET), Mohammed V University, Rabat, Morocco
[2] EuRSED, O2PS scientific production Sarthe France.
[3] Pau University, Pau France.

saad.ennima@gmail.com

ABSTRACT

The objective of this research study based on numerical results is to validate the feasibility and effectiveness of a new method for controlling Hexacopter type UAVs, which belong to the family of multirotor established on laws fractional control (FOC) and to establish a comparison between three types of controllers used to control the attitude of a UAV under different conditions, known as the Hexacopter platform, which is part of the multi-rotor UAV family. The three types of controllers considered in this work are a conventional linear-quadratic LQR controller, the proportional-integral-derivative PID method and a controller based on fractional control laws. The control method asserts advantages regarding of response time and stabilisation at the desired altitude and attitude. This control is intended to be used to control and maintain the desired trajectory during several manoeuvres while minimising energy consumption. The system's performance and stability are analysed with several tests, from simple hovering flight. This new solution applied to multi-rotor UAVs will totally revolutionise this technology in terms of stability and solve the problem for many industries. All the simulations discussed in this article were performed in the MATLAB/Simulink environment.

Keywords: *UAV, Hexacopter, Fractional control, LQR, PID.*

1. INTRODUCTION

This approach deals with the stabilization of an optimized Hexacopter system [16] by the principle of initial state feedback, this law based on fractional control offers a good compromise between the different aerodynamic criteria and the stability performances such as the temporal responses of the system, the accuracy of the displacement of the UAV and the energy consumed by the UAV. In order to succeed in this, it is imperative to take into account in the tests [7] [8] the strength provided or the degree of stability as well as the dimensional parameters internal to the design of the system.

In the last decades, improvements in micro electronic devices, brushless motors, light and powerful LiPo batteries provided an exponential growth and popularity in VTOL UAVs. Quadcopter was the most popular platform at first; however, with the increasing needs of payload, flight time and fault tolerance capabilities, configurations with more than four motors have emerged. Increasing motor number also comes with some drawbacks such as increase in weight, cost, size, etc. At this point, Hexacopter configuration is considered to be a good choice by both industrial and research applications. Hexacopter dynamics is inherently unstable; therefore, it is hard to control the platform without a well-designed controller. There are many works in literature with different control methods such as PID, LQR, adaptive control, Backstepping, fault tolerant control techniques, vision-based control etc. However, works that involve flight test verification are lesser in numbers due to complexities of real time implementation.

In the beginning, the 4-motor UAV was an interesting platform to carry out several aerial missions without human intervention. At the beginning of this technology, the 4-motor UAV was an interesting platform to perform several aerial missions without the intervention of the human being. However, with time, the users require several conditions concerning the UAV's nacelle, the battery autonomy which has a direct link with the UAV's [14] flight time. Adding more motors to the system can also cause disadvantages, such as the weight of the drone which will be higher than the 4 motor configurations, the cost and the external dimensions. For many industrialists and researchers consider that this configuration remains a good choice to solve some problems but it is also necessary to take into account the dynamics of the drone at the stability level because of the added weight and the consumed energy. This is why it is necessary to conceive a robust controller which manages well the energy consumption of the drone. There is a lot of research work already translated into reality for different control methods such as PID [9] [10], LQR [11] [12] [13], etc. However, there is less work on flight test verification due to the complexity of real-time implementation.

In this study, we aim to design a controller never before used for Hexacopter type UAVs in order to see how reliable and efficient it is to have a stable UAV. if this stability condition is automatically validated, we can deduce that the management of the electrical power consumption of our system will be optimised and regulated. the so-called FOC controller is based on fractional control laws. We will study this controller in terms of response time and stabilisation at the desired altitude and attitude. All simulations and tests are generated in MATLAB/Simulink.

The organization of this article is as follows, In the first part, presents the nonlinear equations of the general model of the 6-motor drone, then the representation of the design of the controller based on fractional laws, PID and LQR, under the software matlab, discussion of the results of the simulations made and at the end a conclusion to see the feasibility of this method.

2. DEFINITIONS & ABBREVIATIONS

g : Gravitational acceleration.
m : Mass of hexacopter.
J : Inertia tensor of hexacopter.
cg : center of gravity.
d :Motor centerline to cg. Distance.
K_{dh}: Drag constant for horizontal motion.
K_{dv}: Drag constant for vertical motion.
Fi : Force generated by i_{th} propeller.
Ti : Torque generated by i_{th} propeller.
w_i: Rotational speed of i_{th}motor.
k_f:Electric motor force constant (Fi vs w_i).
k_t:Electric motor torque constant (Ti vs Fi).
$\sum F_{ext}, \sum M_{ext}$: External net forces and moment action on hexacopter cg.
F_g, F_p, F_d: Gravity, Propulsion and Drag forces, respectively.
Mp : Propulsion moment acting on Hexacopter cg.
U: Virtual control input.
k_t: Constant that relates F_i and T_i
$V = [u, v, w]^T$: Hexacopter (body) translational velocity expressed in body frame.
$w = [p, q, r]^T$: Hexacopter (body) angular velocity expressed in body frame.
$R = [x, y, z]$:Position of Hexacopter relative to Earth frame.
$\eta = [\varphi, \theta, \psi]$:Euler angles (Roll, Pitch, Yaw) of Hexacopter.
L_{BE}: Earth to body frame orthogonal transformation matrix.
L_R: Transformation matrix from Euler angle rates to Body angular rates.
U_v: Virtual control input vector.
U_p: Physically realizable control input vector.
X_0: States at hover trim condition.
U_0: Inputs at hover trim condition.
PWM : Pulse Width Modulation.
ESC : Electronic Speed Controller.
MPC : Model Predictive Control.
LQR : Linear Quadratic Control.
PID : proportional integral derivative.
$VTOL$: Vertical Takeoff and Landing.
$c(\cdot)$: Cosine function.
$s(\cdot)$: Sine function.

3. DYNAMIC MODEL OF HEXACOPTER

A dynamical model of hexacopter is obtained by using Newton-Euler equations of motion. 6 DOF equations are very similar to the quadcopter configuration except the control input definitions. First, hexacopter geometry and reference frames used in derivation are described below:

Journal of Theoretical and Applied Information Technology
15th May 2021. Vol.99. No 9

ISSN: 1992-8645 www.jatit.org E-ISSN: 1817-3195

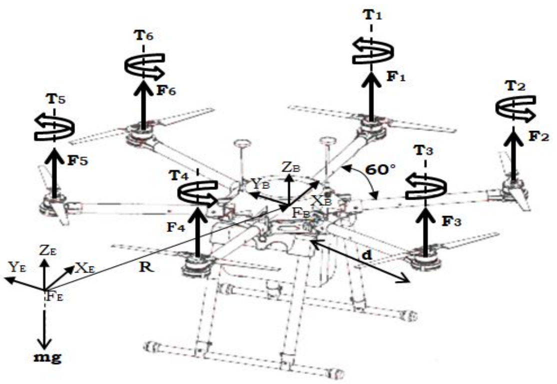

Figure 1: Reference frames, force & torque directions

A. Definition of bearings and parameters of the 6-motor UAV:

Figure 1 shows the design and configuration of the 6-motor UAV used in the study. There are two reference points for the derivation: the first one is the fixed reference point of the Earth base FE which is the non-accelerated inertial reference. the second one FB is the fixed reference but this time linked to the structure of the UAV located at the origin of the center of gravity Cg, which is permanent displacement with the UAV whatever its movement (translation, rotation). The two references and unit vectors are represented in figure 1. For the simulations, the origins of the two references are considered as a single reference at t=0.

B. System inputs and established strategy:

Concerning the Hexacopter drone we have 6 motors in it there are 4 parameters: the angles of Euler (θ,φ,ψ) and the altitude in (z), which are the direct responsible of the controls and followed. For a good interpretation of the results the command U is established in the design of the controller:

$$U = [Fz_c, Mx_c, My_c, Mz_c]^T$$

$$U_r = [F_1, F_2, F_3, F_4, F_5, F_6]^T$$

$$U = PU_r \quad (1)$$

With:

$$P = \begin{bmatrix} 1 & 1 & 1 & 1 & 1 & 1 \\ 0 & -0.87d & -0.87d & 0 & 0.87d & 0.87d \\ -d & -d/2 & d/2 & d & d/2 & -d/2 \\ -k_t & k_t & -k_t & k_t & -k_t & k_t \end{bmatrix}$$

; c = d $\sqrt{3}/2$ = 0.87 d

$$U_r = TU \quad (2)$$

With:

$$T = \begin{bmatrix} 0.167 & 0 & -0.333d & -0.167k_t \\ 0.167 & -1.443 & -0.167d & 0.167k_t \\ 0.167 & -1.443 & 0.167d & -0.167k_t \\ 0.167 & 0 & 0.333d & 0.167k_t \\ 0.167 & 1.443 & 0.167d & -0.167k_t \\ 0.167 & 1.443 & 0.167d & 0.167k_t \end{bmatrix}$$

The given result of the matrix P is found using the above mentioned configuration of the 6-motor UAV in figure 1. U which is the virtual control input composed of Mx_c, My_c, Mz_c, Fz_c which represents the moments in the x y z axes by the rotation of the propellers and the forces generated in the z axes of the UAV. These moments and forces are responsible for the movements of the drone and will be the object of control. This virtual control proposes a physical interpretation of the inputs related to the control and the addition of the integral effect of the controller. this has advantages in the design part of the controller then it is necessary to make a control of the (rpm) angular velocity for each engine of the drone. But we correspond the virtual control input U to the real input control Ur which has a relationship with the angular velocity of the 6 engines.

C. 6-DOF Nonlinear Dynamic Model:

Once the control inputs are defined, the dynamics of the Hexacopter can be generated by considering the external forces and moments acting on the Cg of the Hexacopter. The equations of motion in 6 degrees of freedom are given as follows:

$$\sum F_{ext} = m\dot{V} + w \times (mV_B) \quad (3)$$

$$\sum M_{ext} = m\dot{V} + w \times (Jw) \quad (4)$$

Note that the above equations are expressed in relation to F_B, the fixed reference frame of the UAV.

$\sum M_{ext}$ and $\sum F_{ext}$ are the external moments and forces acting on the 6-motor UAV and the calculation of the $\sum M_{ext}$ is with respect to the center of gravity Cg.

$$\sum F_{ext} = F_{grav} + F_{prop} + F_{drag} \quad (5)$$

$$F_{grav} = -L_{BE}\,[0\ 0\ mg]^T \quad (6)$$

$$F_{prop} = [0\ 0\ F_{z_{total}}]^T \quad (7)$$

$$F_{drag} = -K_d\,[u\ v\ w]^T \quad (8)$$

$$\sum M_{ext} = M_{prop} = [F_{x_{total}}\ F_{y_{total}}\ F_{z_{total}}]^T \quad (9)$$

For the hexacopter drone F_{drag} characterizes the aerodynamic force of the drag, F_{grav} characterizes the force given by the effect of the gravity, concerning the dynamics of the drone is given by the actuators the force and the moment

Journal of Theoretical and Applied Information Technology
15th May 2021. Vol.99. No 9

ISSN: 1992-8645 www.jatit.org E-ISSN: 1817-3195

F_{prop}, M_{prop} which are generated by the system engine plus propeller, With:

$$L_{EB} = \begin{bmatrix} c(\theta)c(\psi) & s(\phi)s(\theta)c(\psi)-c(\phi)s(\psi) & c(\phi)s(\theta)c(\psi)-s(\phi)s(\psi) \\ c(\theta)s(\psi) & s(\phi)s(\theta)s(\psi)+c(\phi)c(\psi) & c(\phi)s(\theta)s(\psi)-s(\phi)c(\psi) \\ -s(\theta) & s(\phi)c(\theta) & c(\phi)c(\theta) \end{bmatrix}$$

$$L_{R} = \begin{bmatrix} 1 & 0 & -s(\theta) \\ 0 & c(\phi) & s(\phi)c(\theta) \\ 0 & -s(\phi) & c(\phi)c(\theta) \end{bmatrix}$$

With the following kinematics the rotational and translational velocities can be developed:

$$\dot{\xi} = [\dot{x}\ \dot{y}\ \dot{z}]^T = L_{EB}[u\ v\ w]^T$$
$$\dot{\eta} = [\dot{\phi}\ \dot{\theta}\ \dot{\psi}]^T = L_R^{-1}[p\ q\ r]^T$$

By combining motion equations, translational and rotational dynamics of hexacopter is obtained [4] [5] as follows:

$$\begin{bmatrix} \dot{u} \\ \dot{v} \\ \dot{w} \end{bmatrix} = \begin{bmatrix} -qw + vr + gs(\theta) - \frac{k_d u}{m} \\ pw - ur + gc(\theta)s(\phi) - \frac{k_d v}{m} \\ -pv + uq - gc(\theta)c(\phi) - \frac{kw}{m} + \frac{F_{z_{act}}}{m} \end{bmatrix}$$

$$\begin{bmatrix} \dot{p} \\ \dot{q} \\ \dot{r} \end{bmatrix} = \begin{bmatrix} qr(I_y - I_z) + M_{x_{act}} \\ qr(I_z - I_x) + M_{y_{act}} \\ qr(I_x - I_y) + M_{z_{act}} \end{bmatrix} \quad (11)$$

<u>Linearized Hexacopter Model:</u>

a. 4-DOF Nonlinear Dynamic Model Used in Linearization:

1) Altitude Dynamics:

Equation (3) gives translational motion of hexacopter in terms of body velocity V. For linearization purposes, we would like to obtain only altitude dynamics in terms of $\ddot{z}$ which is expressed in F_E Equation (12) is obtained after proper algebraic calculations, details of derivation are given in [3]. It is important to note that actuator dynamics is not included in linearization and virtual control input U is used in equations.

Equation (12) gives nonlinear altitude dynamics of Hexacopter expressed in F_E and this equation is used in linearization of altitude dynamics.

$$\ddot{z} = -g + \frac{\cos(\phi)\cos(\theta)F_{z_c}}{m} - k_d\frac{\dot{z}}{m} \quad (12)$$

2) Attitude Dynamics:

Equation (11) gives rotational motion of Hexacopter [18] in terms of body angular rates ω; however, we would like to obtain the same equation in terms of $\ddot{\eta}$. At this point, by making small angle assumption with $\cos() \approx 1$ and $\sin() \approx 0$, following relations are obtained as follows:

$$[p, q, r]^T = [\dot{\phi}, \dot{\theta}, \dot{\psi}]^T \quad (13)$$

$$[\dot{p}, \dot{q}, \dot{r}]^T = [\ddot{\phi}, \ddot{\theta}, \ddot{\psi}]^T \quad (14)$$

Substituting equations (13) and (14) into equation (11) and removing the effects of actuator dynamics for linearization, we obtain equation (15) to express nonlinear attitude dynamics to be used in linearization.

$$\begin{bmatrix} \ddot{\phi} \\ \ddot{\theta} \\ \ddot{\psi} \end{bmatrix} = \begin{bmatrix} \dot{\theta}\dot{\psi}(I_y - I_z) + M_{x_{cmd}}/I_x \\ \dot{\phi}\dot{\psi}(I_z - I_x) + M_{y_{cmd}}/I_y \\ \dot{\phi}\dot{\theta}(I_x - I_y) + M_{z_{cmd}}/I_z \end{bmatrix} \quad (15)$$

b. The inclusion of the state integral in the state space representation:

Our aim was to design a controller that tracks desired altitude and attitude commands. In other words, we want to control states z, φ, θ and ψ. It is also mentioned that the main challenge in LQR and fractional control design is selection/tuning of state and input weight matrices. To simplify this tuning process with physical insight, state space representation is formed in a way that states $(z, \varphi, \theta, \psi)$, derivatives of states $(z', \varphi', \theta', \psi')$ and integrals of states $(\int z\, dt, \int \varphi\, dt, \int \theta\, dt, \int \psi\, dt)$ are all included in state vector X. By considering this, state and input vectors are defined in equation (16), (17).

$$X = [x_1, x_2, \ldots, x_{12}]^T = [\varphi, \dot{\varphi}, \theta, \dot{\theta}, \psi, \dot{\psi}, z, \dot{z}, \int\varphi, \int\theta, \int\psi, \int z]^T \quad (16)$$
$$U = [u_1, u_2, u_3, u_4]^T = [Fz_c, Mx_c, My_c, Mz_c]^T \quad (17)$$

By using equations (12) and (15), the following first order differential equation set is obtained.

$$\begin{pmatrix} f_1 \\ f_2 \\ f_3 \\ f_4 \\ f_5 \\ f_6 \\ f_7 \\ f_8 \\ f_9 \\ f_{10} \\ f_{11} \\ f_{12} \end{pmatrix} = \begin{pmatrix} x_1 \\ x_2 \\ x_3 \\ x_4 \\ x_5 \\ x_6 \\ x_7 \\ x_8 \\ x_9 \\ x_{10} \\ x_{11} \\ x_{12} \end{pmatrix} = \begin{pmatrix} x_2 \\ x_4x_6(I_y - I_z) + M_{x_{roll}}/I_x \\ x_4 \\ x_2x_6(I_z - I_x) + M_{y_{pitch}}/I_y \\ x_6 \\ x_4x_2(I_x - I_y) + M_{z_{yaw}}/I_z \\ x_8 \\ (-mg + \cos(x_1)\cos(x_3))Fz_c - k_d x_8)/m \\ x_1 \\ x_3 \\ x_5 \\ x_7 \end{pmatrix} \quad (18)$$

To obtain the linear equations of the state space, the equations (18) are linearized with respect to a control condition. The matrix A and the matrix B are respectively the equations of the state space. This calculation was done with the Matlab software.
Whatever the value of the altitude for the dynamic model, the matrix A will always be equal to the matrix B, When the hexacopter drone in hover mode, several parameters will be zero, for the reason that equation (18), does not have a coupled nonlinear servo term. Except Fzc is the same as the weight of the UAV.

$$A_{i,j} = \partial f_i/\partial x_j \, , for \; i = 1{:}12, j = 1{:}12 \quad (19)$$
$$B_{i,j} = \partial f_i/\partial u_k \, , for \; i = 1{:}12, j = 1{:}12 \quad (20)$$
$$X_0 = zeros\,(12,1)\,, U_0 = [mg, 0, 0, 0]^T \quad (21)$$

Equation (22) represents the state space dynamics of the 6-motor UAV according to the obtained time-invariant matrix A and matrix B.

$$\Delta X' = A\Delta X + B\Delta U, \; Y = C\Delta X \quad (22)$$

Where:
$\Delta X' = X' - X'_0, \Delta X = X - X_0, \Delta U = U - U_0$

For our trim condition, X_0 and X'_0 are zero vectors; therefore, $\Delta X'$ and ΔX could be replaced with X' and X, respectively.

It is assumed that all states are observable so that C matrix is equal to $I_{12\times12}$.

to move on to the calculation phase, the Matlab calculation software has a calculation platform based on predefined blocks to facilitate the implementation of the script, below is the Simulink matlab representation of the Linear model of the Hexacopter:

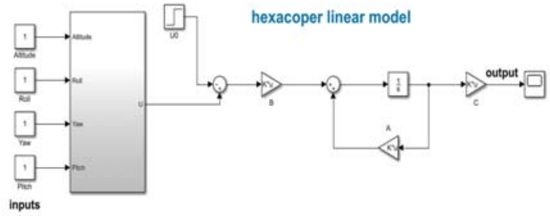

Block diagram 1: Linear model of the Hexacopter in Simulink

4. CONTROLLER DESIGN

A. LINEAR QUADRATIC METHOD:

LQR control is a widely used technique especially for multivariable control problems. It finds optimal gains by solving Algebraic Riccati Equation and the aim is minimizing a predefined cost function. Unlike SISO design approaches like PID with successive loop closure, LQR closes all the loops simultaneously so that tuning of the controller could be done without excessive effort if state and input weight matrices are chosen reasonably.

In this study, our aim is tracking desired values of altitude (z) and attitude (φ, θ, ψ); therefore, we should control error dynamics instead of system dynamics found in equation (22). However, for practical concerns, we would also like to find a constant gain matrix which can be calculated off-line and does not depend on desired states. To satisfy this purpose, cost function that we try to minimize does not include prior knowledge about desired trajectory. It can be given as follows [1]:

$$J = \int_0^\infty ((\Delta X)^T Q \Delta X + ((\Delta U)^T R \Delta U)\, dt \quad (23)$$

where, Q is the state weight matrix and R is the input weight matrix. As it can be seen, cost function is defined by considering the system dynamics given in equation (18).

Solving the Algebraic Riccati Equation that minimizes the cost function defined in equation (23) gives the optimal control gain for regulating the system around design/trim point which is hover condition for our case. However, our aim is tracking and therefore the following error vector is defined to control and minimize the error between desired states (X_d) and actual states (X).

$$e = X - X_d, \; \Delta U = U - U_0 \quad (24)$$

ISSN: 1992-8645 www.jatit.org E-ISSN: 1817-3195

$$\begin{pmatrix} e_1 \\ e_2 \\ e_3 \\ e_4 \\ e_5 \\ e_6 \\ e_7 \\ e_8 \\ e_9 \\ e_{10} \\ e_{11} \\ e_{12} \end{pmatrix} = \begin{pmatrix} \phi - \phi_d \\ \dot{\phi} - \dot{\phi}_d \\ \theta - \theta_d \\ \dot{\theta} - \dot{\theta}_d \\ \psi - \psi_d \\ \dot{\psi} - \dot{\psi}_d \\ z - z_d \\ \dot{z} - \dot{z}_d \\ \int(\phi - \phi_d) \\ \int(\theta - \theta_d) \\ \int(\psi - \psi_d) \\ \int(z - z_d) \end{pmatrix}, U_0 = \begin{pmatrix} mg \\ 0 \\ 0 \\ 0 \end{pmatrix} \quad (25)$$

After defining the error vector, the following control law is used to track desired z, φ, θ and ψ.

$$U = \Delta U + U_0 = -k_i e + U_0 \quad (26)$$

MATLAB "lqr" command which is given in equation (27) is used to solve algebraic Riccati equation and obtain suboptimal gain matrix K. Q and Rmatrices are tuned to achieve desired time domain requirements.

$$[K, S, eig] = lqr(A, B, Q, R) \quad (27)$$

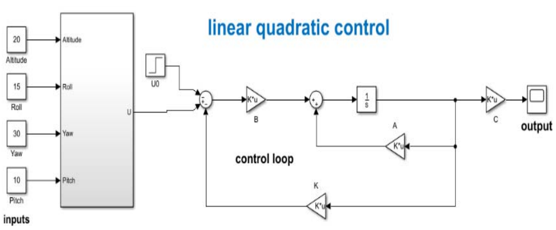

Block diagram 2: LQR control (Simulink model)

B. FRACTIONAL CONTROL METHOD:

In order to establish a fractional controller, the control law for all systems is written as:

$$u(t) = -k x^{(\alpha)}(t) \quad (28)$$

where $\alpha$is a real number representing the order of derivation of $x(t)$.

The equation (22) becomes:

$$x'(t) = Ax(t) - BKx^{(\alpha)}(t) \quad (29)$$

The definition given by Grunwald-Letnikov for a fractional derivative using the Gamma function [2] [3] is:

$$x^{(\alpha)}(t) = \lim_{h \to 0}\left(\frac{1}{h^{(\alpha)}}\right)\sum_{k=0}^{\infty}(-1)^k(\alpha, k)\,x(t - kh) \quad (30)$$

Where $(\alpha, k) = \frac{\Gamma(\alpha + 1)}{\Gamma(k + 1)\Gamma(\alpha - k + 1)}$.

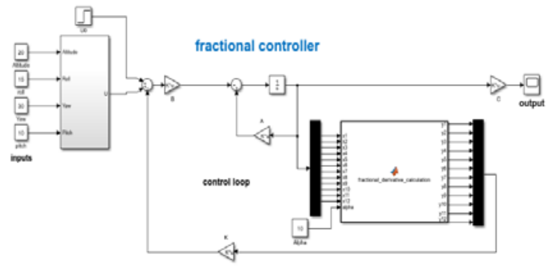

Block diagram 3: fractional controller (Simulink model).

C. PID METHOD (method with block diagram):

The classical PID linear controller has the advantage that parameter gains are easy to adjust, is simple to design and has good robustness. However, some of the major challenges with the hexacopter include the nonlinearity associated with the mathematical model and the imprecise nature of the model due to unmodeled or inaccurate mathematical modeling of some of the dynamics. Therefore, applying a PID controller to the hexacopter limits its performance [6].

Altitude controller:

$$U_1 = K_{p,z}(z - z_d) + K_{d,z}(z' - z'_d) + K_{iz}\int(z - z_d)\,dt \quad (31)$$

Where: z_d is the Desired altitude.

Attitude controller:

$$U_2 = K_{p,\phi}(\phi - \phi_d) + K_{d,\phi}(\phi' - \phi'_d) + K_{i,\phi}\int(\phi - \phi_d)\,dt \quad (32)$$

$$U_3 = K_{p,\theta}(\theta - \theta_d) + K_{d,\theta}(\theta' - \theta'_d) + K_{i,\theta}\int(\theta - \theta_d)\,dt \quad (33)$$

$$U_4 = K_{p,\psi}(\psi - \psi_d) + K_{d,\psi}(\psi' - \psi'_d) + K_{i,\psi}\int(\psi - \psi_d)\,dt \quad (34)$$

Where: ϕ_d ,θ_d and ψ_d are desired roll angle, desired pitch angle and desired yaw angle respectively.

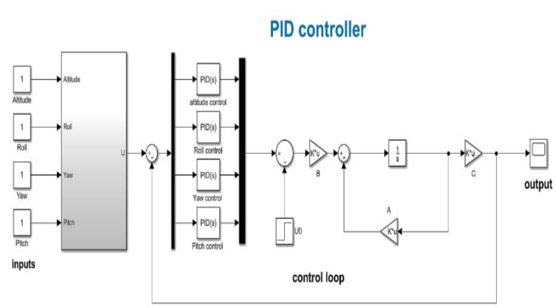

Block diagram 4: PID control (Simulink model).

ISSN: 1992-8645 www.jatit.org E-ISSN: 1817-3195

5. SIMULATION AND COMPATISON:

Table 1: parameters and variables of the hexacopter design needed for the numerical calculation

Par	Definition	value	unit
m	hexacopter mass	15	kg
g	Acceleration of gravity	9.8	m/s^2
k_f	Constant that relates F_i and ω_i	$5.7 \cdot 10^{-8}$	N / rpm^2
k_t	Constant that relates F_i and T_i	0.016	m
Jxx	Hexacopter Inertie Matrix $J = diag(Jxx, Jyy, Jzz)$	1.220	$kg.m^2$
Jyy		1.228	
Jzz		2.065	
d	Distance of motor to center	0.71	m
k_d	Air-torque Coef.by torque dividing rotation-speed²	$7.245e-2$	$N.m/(rad/s)^2$

After linearization, time-invariant A, B, C matrices are found as follows:

$$A = \begin{bmatrix} 0 & 1 & 0 & 0 & 0 & 0 & 0 & 0.0000 & 0 & 0 & 0 & 0 \\ 0 & 0 & 0 & 0 & 0 & 0 & 0 & 0.0000 & 0 & 0 & 0 & 0 \\ 0 & 0 & 0 & 1 & 0 & 0 & 0 & 0.0000 & 0 & 0 & 0 & 0 \\ 0 & 0 & 0 & 0 & 0 & 0 & 0 & 0.0000 & 0 & 0 & 0 & 0 \\ 0 & 0 & 0 & 0 & 0 & 1 & 0 & 0.0000 & 0 & 0 & 0 & 0 \\ 0 & 0 & 0 & 0 & 0 & 0 & 0 & 0.0000 & 0 & 0 & 0 & 0 \\ 0 & 0 & 0 & 0 & 0 & 0 & 0 & 1 & 0 & 0 & 0 & 0 \\ 0 & 0 & 0 & 0 & 0 & 0 & 0 & -0.0048 & 0 & 0 & 0 & 0 \\ 1 & 0 & 0 & 0 & 0 & 0 & 0 & 0.0000 & 0 & 0 & 0 & 0 \\ 0 & 0 & 1 & 0 & 0 & 0 & 0 & 0.00000 & 0 & 0 & 0 & 0 \\ 0 & 0 & 0 & 0 & 1 & 0 & 0 & 0.00000 & 0 & 0 & 0 & 0 \\ 0 & 0 & 0 & 0 & 0 & 0 & 1 & 0.00000 & 0 & 0 & 0 & 0 \end{bmatrix}$$

$$B = \begin{bmatrix} 0.0000 & 0 & 0 & 0 \\ 0 & 0.8143 & 0 & 0 \\ 0 & 0 & 0 & 0 \\ 0 & 0 & 0.8143 & 0 \\ 0 & 0 & 0 & 0 \\ 0 & 0 & 0 & 0.4843 \\ 0 & 0 & 0 & 0 \\ 0.0667 & 0 & 0 & 0 \\ 0 & 0 & 0 & 0 \\ 0 & 0 & 0 & 0 \\ 0 & 0 & 0 & 0 \\ 0 & 0.0000 & 0.0000 & 0.0000 \end{bmatrix}$$

$C = I_{12 \times 12}$

$Q = diag([1, 0.12, 1, 0.12, 2, 0.24, 1, 0.12, 1, 1, 1, 1])$

$R = diag([1\ 1\ 1\ 1]);$

$$K_{lqr} = \begin{bmatrix} 0.00 & 0.00 & 0.00 & 0.00 & 0.00 & 0.00 & 5.07 & 12.26 & 0 & 0 & 0 & 1 \\ 2.44 & 2.47 & 0.00 & 0.00 & 0.00 & 0.00 & 0.00 & 0.000 & 1 & 0 & 0 & 0 \\ 0.00 & 0.00 & 2.44 & 2.48 & 0.00 & 0.00 & 0.00 & 0.000 & 0 & 1 & 0 & 0 \\ 0.00 & 0.00 & 0.00 & 0.00 & 9.02 & 9.57 & 0.00 & 0.000 & 0 & 0 & 1 & 0 \end{bmatrix}$$

Results and discussions:

1- PID control:

Figure 2 and figure 3 represent the altitude and altitude response of the hexacopter at $t = 10s$.

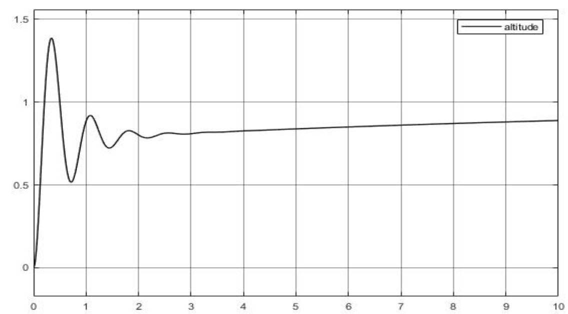

Figure 2: altitude response at t = 10sec

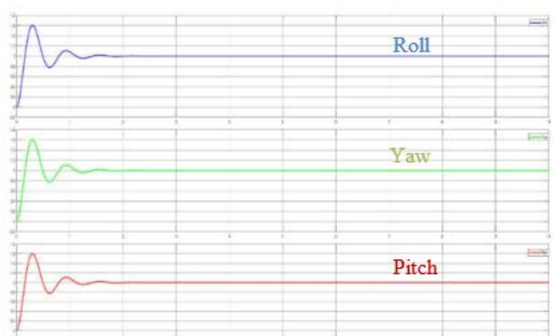

Figure 3: attitude response at t=10sec

For better understanding we studied the steady state error at 150s to see if the controller reaches the final value. Results are displayed in figure 4 and 5.

ISSN: 1992-8645 www.jatit.org E-ISSN: 1817-3195

Figure 4: altitude steady state error at t=150sec

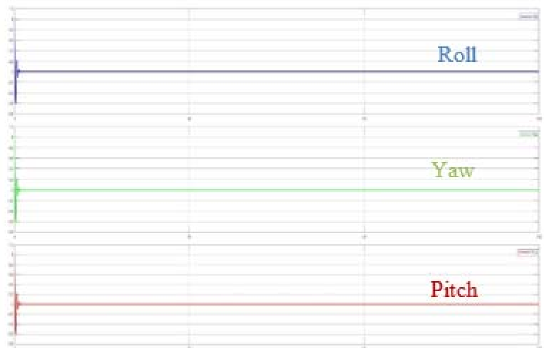

Figure 5: attitude steady state error at t = 150sec

As can be seen in Figures (3) and (5), tracking attitude performance is satisfactory, the system response is fast, and the steady state error after stabilization is null. For the altitude control, although the system response was fast, it couldn't compensate the heavy weight of the Hexacopter faster enough. After stabilization, the steady state error is null due to the integration part of the controller, but increasing the I term of the PID may cause the system to oscillate even more.

2- LQR control:

Same tests are used and under the same condition to compare performances between the PID and LQR control.

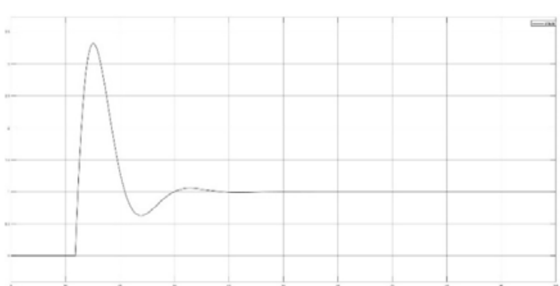

Figure 6: altitude response at t = 100sec

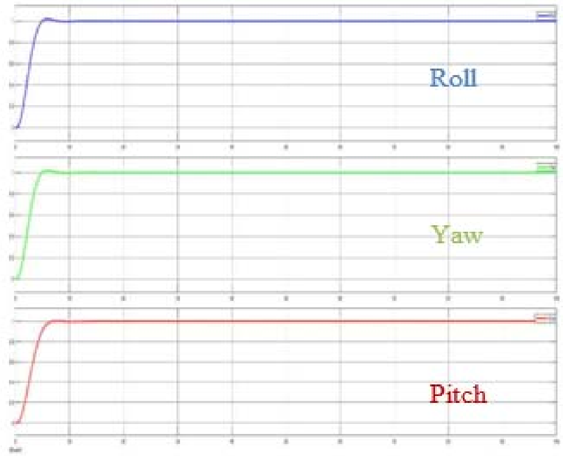

Figure 7: attitude response at t = 100sec

From the results above, we can see that the LQR controller is slower, but it gave better results in term of stabilization, reaching final high is better with LQR controller and the steady state error converge to zero as it can be seen in figures (8) and (9).

Figure 8: altitude steady state error at t=150sec

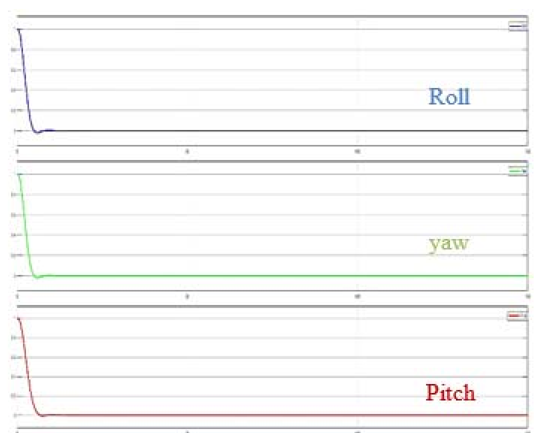

Figure 9: attitude steady state error at t=150sec

Journal of Theoretical and Applied Information Technology
15th May 2021. Vol.99. No 9

ISSN: 1992-8645 www.jatit.org E-ISSN: 1817-3195

Overall, the PID controller was faster but it oscillates and doesn't eliminate altitude steady state error easily unlike the LQR controller that despite its response time, it was very stable and gave better altitude response.

3- Fractional control:

A. fractional control law in state space:

We have $$u(t) = -kx^{(\alpha)} \quad (35)$$

For different values of α and as a function of time we studied the behaviour of the Euler angles under Matlab and Simulink software, as shown in the following figures:

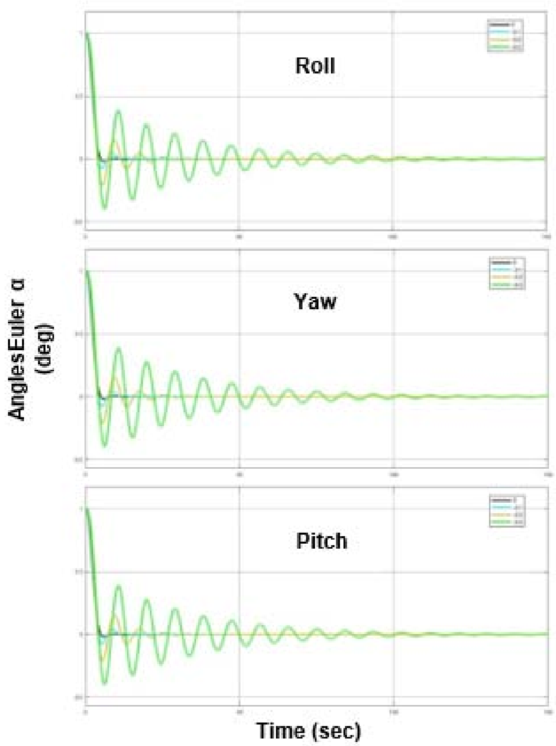

Figure 10: As a function of t=150s, the Angles Euler Roll, Yaw, Pitch, the variation of α from 0 to -0.3 with a step of 0.1

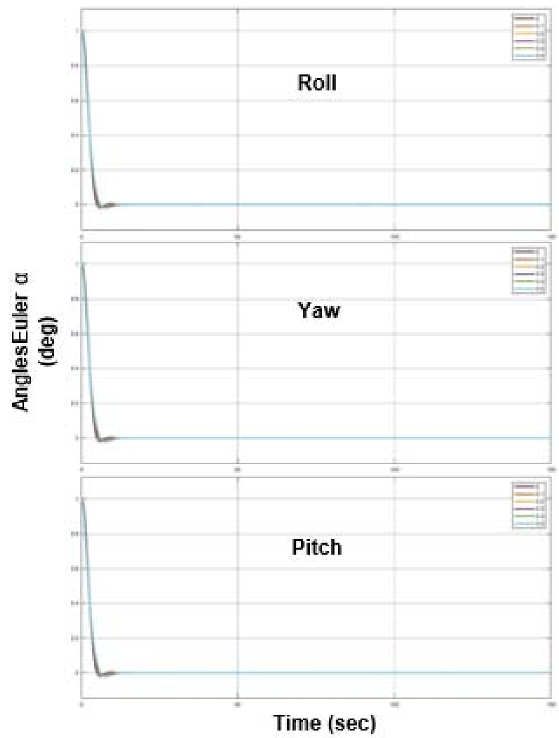

Figure 11: As a function of t=150s, the Angles Euler Roll, Yaw, Pitch, the variation of α from 0 to 0.5 with a step of 0.1)

Negative values of α in the simulation introduce a robust fractional integrator which provides a faster response to the system, but has an impact on the stability i.e. it consumes more energy.

For positive values of α, the system is more stable than for negative values of α and consumes less energy and the steady state error decreases. For this reason, the choice of α depends on the experiment.

To highlight the energy saving or rather consumption, 150sec for each α was plotted to see the control action that related to the reaction wheels.

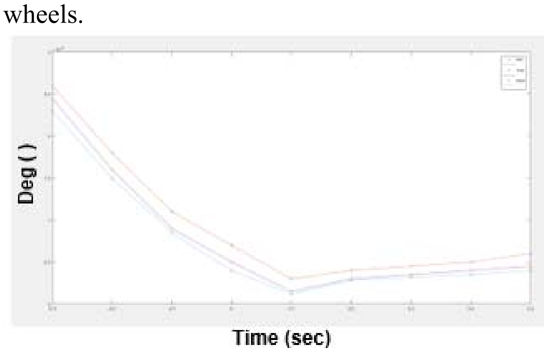

Figure 12: Action control for each α (Roll, Yaw and Pitch)

ISSN: 1992-8645 www.jatit.org E-ISSN: 1817-3195

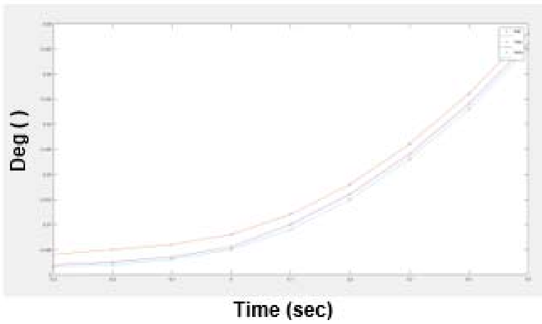

Figure 13: steady state errors at t = 150s (Roll, Yaw and Pitch)

At α = 0.1 for Roll, Yaw and Pitch. Figure (12) illustrates that the curves have a parabolic behaviour.

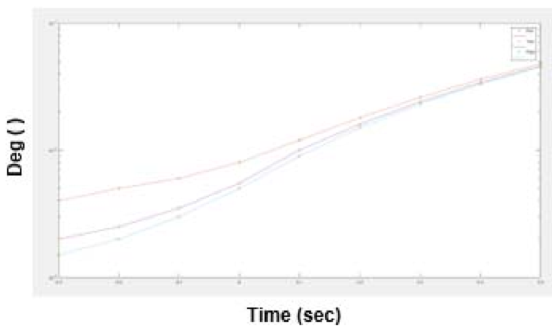

Figure 14: At t = 150s, representation of the error in steady state.

Figure (13) shows the shape of the curves which indicates that the accuracy is good for negative values of α. In logarithmic scale, (SSE) the steady state error changes exponentially with α > 0:

$$SSE = \exp(k.\alpha) \; ; \; k \approx \frac{0.03 - 0.01}{0.3 - 0.1} = 0.1$$

B. Proportional fractional derivative:

The last point revealed that control fractional is more exact. However, it consumes more energy unlike the values of α > 0 there is a noticeable loss in the quality of accuracy, but on the other hand the energy consumption has been reduced.

To solve this problem and minimize the energy consumption without affecting the accuracy, the following fractional control law is given below:

$$u(t) = -K_1 x_1 - K_2 x_2^{(\alpha)}$$

Where:

$$x_1 = (\phi, \theta, \psi)^T \; and \; x_2 = (\dot{\phi}\ , \dot{\theta}, \dot{\psi})^T$$

The following tests in the figure below represent the angular velocities versus time with t= 150sec of the Euler angles (Roll, Yaw and Pitch), for variations of the value of α, from -0.2 to the value 0.3 with a step equal to 0.1. A variety of colors has been implemented for the good understanding and shown the quality of the curves. After all the calculation done, a remark has been made concerning this fractional derivative control law. That it gathers with the $PD^{(1+\alpha)}$ control law.

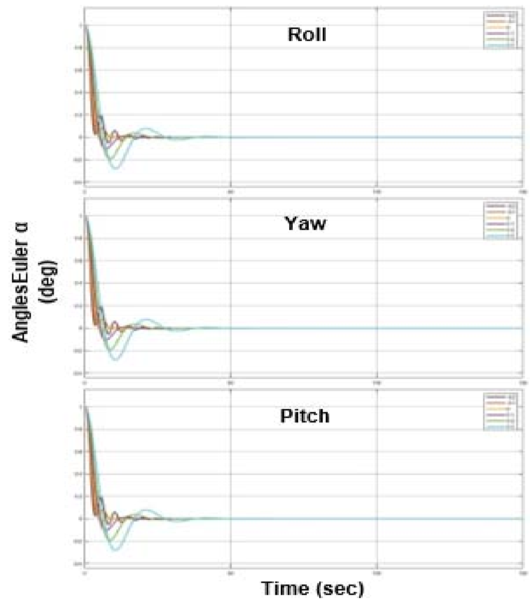

Figure 15: As a function of t=150s, the angle of Roll, Yaw, Pitch, (variation of α from -0.2 to 0.3 with a step of 0.1) according to the derived fractional control law.

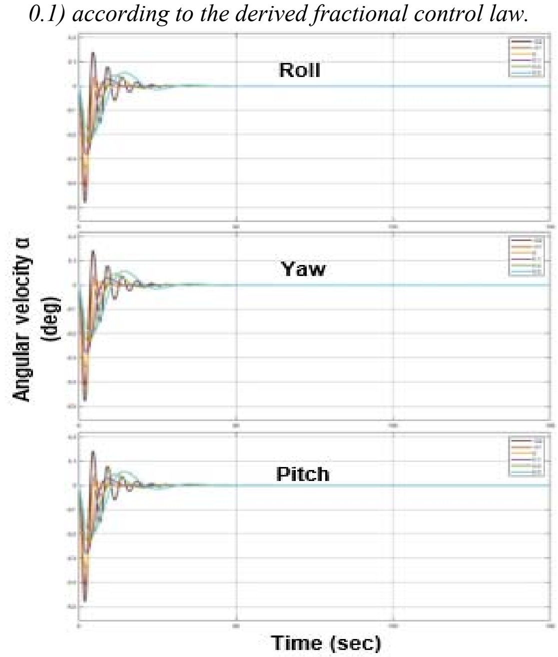

Figure 16: As a function of t=150s, the Roll, Yaw, Pitch angular velocity, (variation of α from -0.2 to 0.3 with a step of 0.1) according to the derived fractional control law.

Journal of Theoretical and Applied Information Technology
15th May 2021. Vol.99. No 9

ISSN: 1992-8645 www.jatit.org E-ISSN: 1817-3195

As the value of α increase from -0.2 to 0.3, there is an effect on the stability of the system which makes it more accurate, which can also be seen in the graphs showing the angular parameters of the velocity for Roll, Yaw and Pitch.

From the above figures, it should be mentioned that from the interpretation of the results in findings that the relative coefficient a α represents the role of a damping coefficient of the 6-motor UAV system. Figure (17) and figure (18) illustrate the response of the roll angle, which is part of the Euler angles, as a function of the time that the choice has been set to 150s. It can also be seen that the drone system is overdamped for the reason that the tolerance band is a ±0.05° and the lower limit is -0.05. For values of α which are in the vicinity of 0.4, so it can be concluded that the system behaves like a 1st order system. This means that it is only necessary to change the value of α for the UAV Hexacopter system [17] to be damped without having any change in the gain matrix.

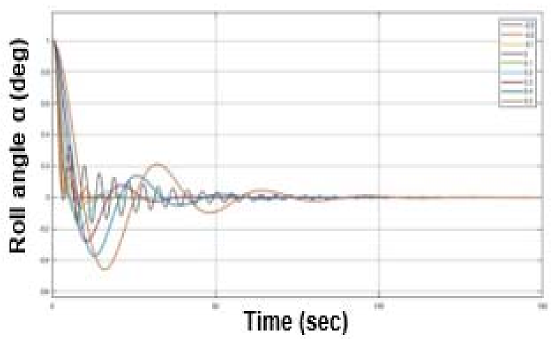

Figure 17: As a function of t=150s, the angle of Roll, (the variation of α from -0.3 to 0.5 with a step of 0.1) according to the derived fractional control law.

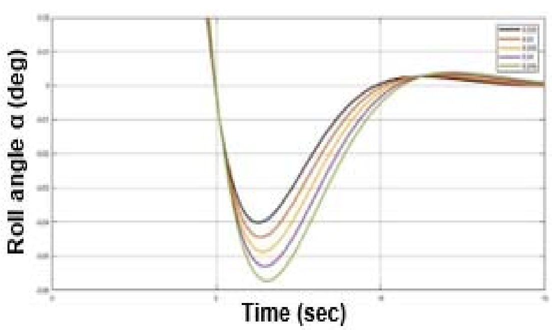

Figure 18: As a function of t=15s, overshoot for α = 0.04, (the variation of α from -0.025 to 0.045 with a step of 0.005)

C. Fractional derivative $P^{(\alpha)}$**D:**

The control law is given by:

$$u(t) = -K_1 x_1^{(\alpha)} - K_2 x_2$$

Where:

$$x_1 = (\phi, \theta, \psi)^T \ and \ x_2 = (\dot{\phi}, \dot{\theta}, \dot{\psi})^T$$

The same behavior of the system is observed. Next figures give Euler angle [19] [20] versus time in addition to the angular velocities for different values of α.

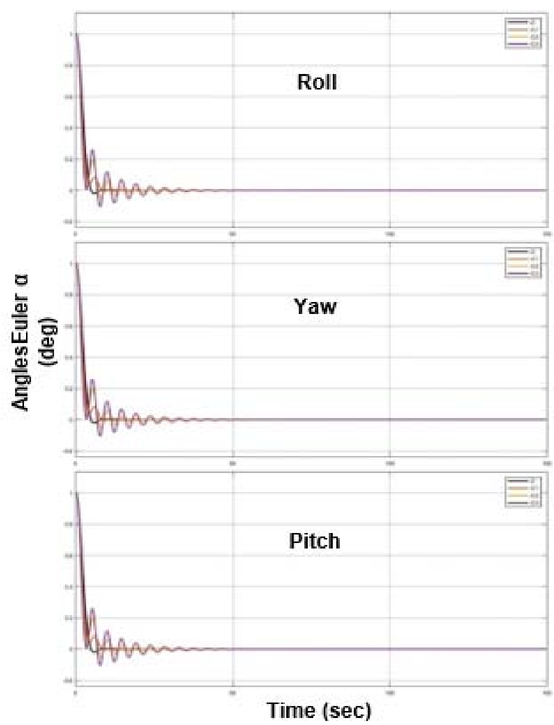

Figure 19: As a function of t=150s, the angle of Roll, Yaw, Pitch (the variation of α from -0.3 to 0 with a step of 0.1) according to the derived fractional control law $P^{(\alpha)}D$.

ISSN: 1992-8645 www.jatit.org E-ISSN: 1817-3195

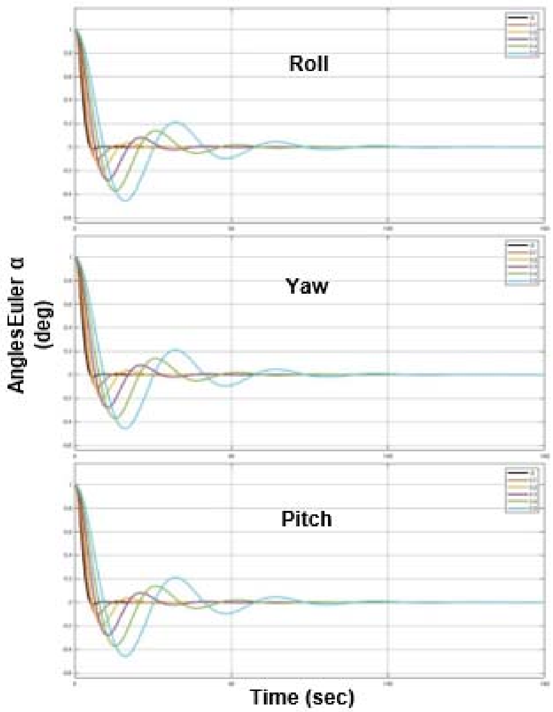

Figure 20: As a function of t=150s, the angle of Roll, Yaw, Pitch (the variation of α from 0 to 0.5 with a step of 0.1) according to the derived fractional control law $P^{(\alpha)}D$.

From the above figures the fractional control law $P^{(\alpha)}D$ is more accurate than the other fractional control laws studied, the interpretation of this accuracy is obtained by the integral term $P^{(\alpha)}$ for α values < 0.

The interpretation of the previous control law in terms of the positive variation of the stabilisation as a function of time goes through discontinuities. this is generated at the time of the undershoots and overshoots that reach the lower and upper limit.

For the first fractional controller, there is a minimum of action of the reaction wheel control which has been achieved for the value of α = 0.1. also for the tolerance band which is lower than that of the steady state error. For all the tests carried out in the steady state simulations the best error marked for α equal to -0.3.

Concerning the second fractional controller (PROPORTIONAL FRACTIONAL DERIVATIVE), the stabilisation time improved for minimum values of α = 0.4 and above, also the control action of the reaction wheels increases slightly.

In the third controller $P^{(\alpha)}D$ the integral part was introduced. For the purpose of further decreasing the stabilization response time, the minimum of the control reaction [15] was reached and the stabilization time of the Hexacopter drone system was reduced, with a minimum obtained of α = -0.25 in Roll with a slight increase of the power consumption.

6. CONCLUSION

In this paper, we built a dynamic model for an unmanned aerial vehicle UAV “hexacopter” and implement three types of controller: PID control, LQR control and fractional controller to study its advantages in terms of response time, stabilization, settling time and energy using.

To have reasonable comparisons, tests are taken under the same conditions. The linear model is generated using MATLAB environment. All the controllers are tested by using the same model also built in MATLAB/Simulink.

All of the three different control methods presented satisfactory but different results; the PID controller had fast response time but when trying to eliminate the steady state error the system started to oscillate. For the LQR control, the controller was robust and produced a very low steady state error, but with a big transition delay and slow settling time. That is why a third controller was used. The three Fractional controllers take the advantages of the LQR one with a much faster settling time.

In the bibliography several different control methods for autonomous systems have proven to have great potential and have provided interesting results, but each one has advantages as well as disadvantages, for example the PID controller, which has a good characteristic regarding the response time which is fast, but trying to eliminate the error in steady state it allows the system to start oscillating. Another example of a controller known as LQR, among its characteristics is a robust design that produces a very low steady state error, but with a slow response time. For this reason, this paper is interested in the implementation of the method newly known as FOC, i.e. fractional order controller, with the objective of finding a solution that solves this compromise between the system's stabilization time and the energy consumed. The three fractional controllers presented take advantage of the LQR control method with the characteristic of having a fast settling time.

The results presented in this article show that the application of the fractional controller can provide satisfactory control in terms of the attitude of the hexacopter system. If all the parameters are

ISSN: 1992-8645 www.jatit.org E-ISSN: 1817-3195

correctly defined and the choice of weighting matrices correctly established, the controller can be implemented on an on-board system with satisfactory results in most desired flight situations.

The contribution of the adaptation of this fractional controller is to have reduced and optimized energy consumption. In fact, applying the FOC controller results in implicit energy optimization. Furthermore, introducing a new criterion that forces the controller to alter performance in order to extend the mission duration is another level of optimization.

The results and simulation done in this paper as a whole prove that this fractional controller is a more flexible controller compared to the existing controller by giving better results in terms of response time and accuracy. In addition, other dynamic properties such as damping effects can be adjusted using this controller.

REFERENCES :

[1] Suicmez E.C. and Kutay A.T. (2017) Attitude and Altitude Tracking of Hexacopter via LQR with Integral Action, International Conference on Unmanned Aircraft Systems (ICUAS), Miami, FL, USA, June 2017

[2] A. Kailil, N. Mrani, M. Abid S. Choukri1, M. Mliha Touati, N. Elalami "Fractional Regulators For Spacecraft Attitude Stabilization".

[3] Taha Ennaciri, Nabil Mrani, Ahmed El abbassi and Jaouad Foshi "Attitude Control of a Quadcopter Platform Based on Fractional Control Laws".

[4] Mostafa Moussid, Adil Sayouti, Hicham Medromi "Dynamic Modeling and Control of a HexaRotor using Linear and Nonlinear Methods".

[5] S. Omari, M.D. Hua, G. Ducard and T. Hamel," Hardware and Software Architecture for Nonlinear Control of Multirotor Helicopters", IEEE/ASME Transactions on Mechatronics, vol.18, no.6, pp. 1724-1736, December 2013.

[6] A. Alamio, V. Artale, C. Milazzo, A. Ricciardello, L. Trefiletti," PID Controller Applied to Hexacopter Flight", Journal of Intelligent and Robotic Systems, vol.72, no.2, pp. 1724-1736, November 2013

[7] Saad. Ennima, A. El Gharad, S. Bourekkadi, Z. Mouammine, T. El Ajraoui. (2020) "Optimization of the choice of parameters and performance analysis of the design of a hexacopter uav dedicated to precision agriculture in Morocco". Journal of Advanced Research in Dynamical and Control Systems.

[8] Valentin-Charbonnel C , Duc G. and Le Ballois S, Low-Order Robust Attitude Control of an Earth Observation Satellite, Control Engineering Pactice 7 (1999) 493-506.

[9] Sidi M. J., Spacecraft Dynamics and control, Cambridge University Press, Cambridge, UK, 1997.

[10] Witfond C, Forrest D, The CATSAT Attitude Control systel, Proceeding of the 12th Annual AIAA/USU Conference on small Satellite, 1996.

[11] Musser K.L, Elbert W.L, Autonomous Space Attitude Control using Magnetic Torquing only, Proceeding of flight mechanics estimation theoty symposium, NASA.

[12] Seunghee Yu, Jinyeong Heo, Jinyeong Heo, Sekyung Jeong, Yongjin Kwon, Technical Analysis of VTOL UAV, January 2016Journal of Computer and Communications 04(15):92-97

[13] Emre Can Suicmez; Ali Turker Kutay. Attitude and altitude tracking of hexacopter via LQR with integral action. 2017 International Conference on Unmanned Aircraft Systems (ICUAS)

[14] Akash Maity, Koustav Roy. Conceptual Design of a Special Autonomous VTOL Drone. Mar 2018 AISSEC-2018, Department of Metallurgical and Materials Engineering

[15] Julio Alberto Mendoza-Mendoza, Victor Javier Gonzalez-Villela, Carlos Aguilar-Ibáñez, Leonardo Fonseca-Ruiz. Control of Drones. Feb 2021Drones to Go.

[16] Slimani, K., Bourekkadi, S., Messoussi, R., Ruichek, Y., & Touahni, R. (2020, June). Sharing Emotions in the Distance Education Experience: Attitudes and Motivation of University Students. In 2020 International Conference on Intelligent Systems and Computer Vision (ISCV) (pp. 1-10). IEEE.

[17] B VenkataB. Venkata Mounish Reddy. potential applications of drones. Vol. 5 Special lssue January 2021 E-ISSN: 2456-5571.

[18] Shruti Goyal, Drone Technology: A boon with a mission. Article ,Jan 2021

[19] K Ramesh, B Priya Dharshini, K Haridass. Sanitization using Hexacopter Autonomous Drone. February 2021IOP Conference Series Materials Science and Engineering 1059(1):012043

ISSN: 1992-8645 www.jatit.org E-ISSN: 1817-3195

[20] Landis Markley, John Crassidis. Euler Angles, DOI: 10.1007/978-1-4939-0802-8_9 In book: Fundamentals of Spacecraft Attitude Determination and Control
[21] Aleix Rull Sanahuja, Federico ThomasFederico Thomas. On Generalized Euler Angles. New Trends in Mechanism and Machine Science. New Trends in Mechanism and Machine Science.
[22] Zubareva, E. A., Basantsov, I. V., Byelov S. V. (2020). Financial e-control: modernization of the state financial control system in the conditions of digital economy. Journal of Automation and Information Sciences. 52(10), 62-75